e-Jurnal Sains Nuklear Malaysia, 2022, Vol. 34: 37 – 49
eISSN: 2232-0946

RADIATION-INDUCED RAFT COPOLYMERIZATION AND CROSSLINKING OF PALM OIL-BASED BLOCK COPOLYMERS NANOPARTICLES

Rida Tajau[1], Rosiah Rohani[2], Wan Nor Roslam Wan Isahak[2] and Mek Zah Salleh[1]

[1]Radiation Curing and Synthesis Group, Radiation Processing Technology Division, Malaysian Nuclear Agency, 43000 Kajang, Selangor, Malaysia
[2]Department of Chemical and Process Engineering, Faculty of Engineering and Built Environment, Universiti Kebangsaan Malaysia, 43600 UKM Bangi, Selangor, Malaysia
Corresponding author: rida@nuclearmalaysia.gov.my ; rosiah@ukm.edu.my

ABSTRACT

The polymeric nanoparticles (NPs) with desirable structures and properties extracted from palm oil by using the gamma radiation-induced reversible-addition fragmentation chain transfer (RAFT) polymerisation and crosslinking technique. The raw materials of acrylated palm olein (APO) and polyol ester were used to create nanoparticle-based drug delivery systems. The gamma radiation-induced RAFT offers a promising method to produce NPs *with size of less than 150 nm and low molecular weight of 23,982 Da. The crosslinked poly(APO-b-polyol ester) copolymer* NPs *was determined as biodegradable, amorphous, and had good thermal properties as assessed by FTIR, XRD, DSC and TGA analyses. The discovery implied that radiation processing technology could be used to prepare and obtain the desired nanocarriers.*

Keywords: gamma radiation; nanoparticles; palm oil; RAFT; drug delivery system

INTRODUCTION

The polymeric NPs are gaining interest in medical applications due to their unique features, such as larger functional surface area for binding proteins, favourable quantum properties, and the ability to adsorb, carry, and release therapeutic ingredients. These inherent properties are collectively engineered to form polymeric NPs for drug delivery systems, which are specifically applied to target, diagnose, and treat diseases in the human body.

Many research works have applied RAFT polymerisation for the development of polymeric nanomaterials by using gamma radiation (Bowes, 2007; Chen & Seko, 2017; Chiefari et al., 1998; Meléndez-Ortiz et al., 2015; Millard et al., 2010; Moad et al., 2006; Quinn et al., 2007; Stenzel, 2008; Tian et al., 2018; Guven, 2021). Gamma radiation as an initiation source is considered as one of the most powerful tools for generating radicals in RAFT polymerisation (Ashfaq et al., 2020; Barsbay & Guven, 2020). The application of this process offers various advantages, such as easy set-up, inexpensive, less toxic, and an environmentally-friendly process. In addition, gamma radiation is widely applied in radiation processing for the polymerisation, crosslinking, grafting, interpenetrating polymer networks, and modifying polymers (Barner et al., 2003; Flores-Rojas, 2020; IAEA 2002, 2004, 2010; Meléndez-Ortiz et al., 2015; Quinn et al., 2007; Rosiak et al., 2002; Tajau et al., 2017; Ulanski & Rosiak, 1999).

This study had attempted to synthesise the poly(APO-*block*-polyol ester) NPs of palm oil-based polymers of acrylated palm olein (APO) (Tajau et al., 2020) and polyol ester (Tajau et

al., 2018) via the gamma radiation induced-RAFT polymerisation and crosslinking processes. Therefore, the effectiveness of the low-dose gamma irradiation-induced-RAFT polymerisation on the synthesis of potential drug carriers copolymer NPs with size of less than 150 nm; is thus expected to be demonstrated from the physiochemical and morphological properties that will be investigated by dynamic light scattering (DLS), field emission scanning electron microscopy (FESEM), Fourier transform near-infrared (FT-NIR) spectrometer, transmission electron microscopy (TEM), gel permeation chromatography (GPC). Also, the characterisation through thermogravimetric analyser (TGA), the differential scanning calorimetry (DSC) and that of the X-ray powder diffraction (XRD).

MATERIALS AND METHODS

Materials

Acrylated palm olein (APO) and polyol ester were synthesised in the Laboratory of Radiation Curing and the Synthesis Group (KSPS), Radiation Processing Technology Division (BTS), Agensi Nuklear Malaysia, Selangor, Malaysia. N,cetyl-N,N,N-trimethylammonium bromide (CTAB) (98%, Merck), S,S-dibenzyl trithiocarbonate (DBTTC) (97%, Aldrich), ethyl acetate (EA) (99.5%, Merck), and n-heptane (99.99%, Fisher) were used as received without further purification. Ultrapure water (Millipore system) was used throughout the experiments. All samples were irradiated by using gamma radiation from Cobalt-60 source at Research Loop, Sinagama Irradiation Facility (Agensi Nuklear Malaysia), Selangor, Malaysia.

Formation of poly(APO-*b*-polyol ester) nanoparticles

The macro-APO-RAFT agent solution was prepared by mixing 180 mg of APO, 3 mg of DBTTC, 1ml of EA, and 100 ml of CTAB micelles solution. The mixture was stirred at 300 revolution per minute (rpm) for 24 h. Then, the sample was continuously stirred by using a high-speed disperser (model: Dispermat, VMA-Getzmann) at 3000 rpm for 1 h. Next, the samples were degassed by using nitrogen gas for 30 min and tightly capped before exposed to the gamma (ɣ) radiation at 500 Gy and 700 Gy with a dose rate of 2.16 Gy/s.

The poly(APO-*b*-polyol ester) NPs was prepared from 1 mg of DBTTC, 0.3 ml of EA, 3 mg of polyol ester and 20 ml of macro-APO-RAFT agent solution. The mixture was initially stirred at 300 rpm for 1 h with a magnetic stirrer before continuing with another hour of stirring at 6,000 rpm. Once the mixtures had undergone a nitrogen degassing process, they were exposed to a range of gamma radiation doses of 100 Gy, 400 Gy, 700 Gy and 1 kilogray (kGy), 5 kGy and 10 kGy. The NPs were purified and dried by using the dialysis membrane and lyophilisation techniques.

Physicochemical and thermal properties

The hydrodynamic mean diameter (nm) of the samples was determined by photon cross-correlation spectroscopy (PCCS) with a helium-neon (HeNe) laser at a wavelength of 632 nm by using DLS (Sympatec Nanophox, German). The macro-APO radicals concentration and molecular weights transformations were analysed against the radiation dose by using a UV-Vis spectrophotometer (Shidmazu UV-1800) and GPC (Waters). The amount and percentage of reactants conversion to macro-APO agent and NPs were calculated by using Equation 1 to Equation 7. The unreacted concentration of the monomer was calculated by using Equation 1 and Equation 3, which were taken from the calibration curve of the APO in n-heptane at wavelength of 210 nm and the DBTTC in ethyl

acetate at wavelength of 350 nm. Then, the reacted concentration of APO and DBTTC were calculated by using Equation 2 and Equation 4, respectively:

$$y = 9970.8x \quad \text{(Eq. 1)}$$

$$\text{Concentration of macro} - \text{APO} - \text{RAFT radicals} = a - b \quad \text{(Eq. 2)}$$

Where, a is initial concentration of monomer in molar and b is unreacted monomer concentration in molar at absorbed dose.

$$y = 672.57x \quad \text{(Eq. 3)}$$

$$\text{Concentration of DBTTC} = a - b \quad \text{(Eq. 4)}$$

Where, a is initial concentration of monomer in molar and b is unreacted monomer concentration in molar at absorbed dose.

The unreacted APO concentration was determined by using Equation 1 to measure its excess weight. The APO actual weight and percentage conversion to NPs were determined by using Equation 5 and Equation 6 from the obtained excess weight value.

Actual weight of monomer for NPs development:

$$= \text{Initial weight of monomer} - \text{Excess weight of monomer after irradiation} \quad \text{(Eq. 5)}$$

Conversion percentage of monomer to NPs:

$$= \frac{\text{Weight of monomer used after irradiation}}{\text{Weight of initial monomer}} \text{ x } 100 \quad \text{(Eq. 6)}$$

At wavelength of 360 nm, the unreacted polyol ester absorbance peak in acetone was selected and its concentration was calculated by using Equation 7. The obtained concentration value was then used to determine the actual weight and conversion percentage of the polyol ester used in the manufacture of NPs by using Equation 5 and Equation 6. The production yield of NPs was calculated by using Equation 8.

$$y = 426.53x \quad \text{(Eq. 7)}$$

Nanoparticle yield : (Eq. 8)

$$= \frac{\text{Actual weight of product}}{\text{Weight of (macroAPO} + \text{Polyol ester} + \text{DBTTC)}} \text{ x } 100$$

The Jeol electron microscope (Japan) at voltage of 160 kV and the Zeiss Gemini SEM500 electron microscope (German) at voltage of 1 kV were used to analyse the TEM and FESEM images of the NPs. Infrared (IR) spectra of the samples were analysed by using Spectrum 400, FT-NIR spectrometer (Perkin Elmer, UK). IR spectra of the samples were obtained by using a diamond attenuated total reflectance (DATR) technique and the IR spectra were recorded in the range of 4000 cm^{-1}–500 cm^{-1}. The in-vitro degradation of the NPs was performed with simulated body fluid (SBF) solution in an incubator (Delta, DLS-100) at 37 ^{o}C with orbital shaking at 150 rpm for a set period of 30 days, 60 days, and 90 days. The TGA model TGA-SDTA 851e Mettler Toledo (USA) was used to study the thermal decomposition property of the samples at temperatures from 27 °C to 800 °C and heated at a rate of 10 °C/min in nitrogen gas atmosphere. The DSC analyser (model DSC 822 Mettler Toledo,

USA) was used to study the thermal properties of the samples at the heating and cooling cycle temperatures from -50 °C to 200 ºC at a rate of 10°C/min under nitrogen atmosphere. The XRD measurement was carried out by using a PANalytical PW3040/60 X'Pert PRO apparatus (Netherlands) to obtain the XRD spectra. The crystallinity index (CI) percentage of the sample was calculated by using the XRD deconvolution method utilising a curve-fitting process. The calculation by using Equation 9 as follows:

$$\mathrm{CI}, \% = \frac{S_c}{S_t} \text{ x } 100 \qquad \text{(Eq. 9)}$$

Where, S_c is area of the crystalline domain and S_t is area of the total domain.

RESULTS AND DISCUSSION

Radiation synthesis of poly(APO-*b*-polyol ester) nanoparticles

The mechanism of RAFT polymerisation under gamma radiation in the formation of block copolymer is shown in Figure 1. The poly(APO-*b*-polyol ester) NPs were produced by adding polyol ester (second monomer) into the macro-APO-RAFT agent system. The intermolecular crosslinking process dominated the recombination of molecules in the formation of the poly(APO-*b*-polyol ester) NPs that led to particle size increase (IAEA, 2010; Ulanski & Rosiak, 2004).

The use of FTIR spectroscopy to observe the formation of poly(APO-*b*-polyol ester) NPs verified the appearance of main compound of NPs, such as an amine (C-N) functional group at wavelengths between 1000 cm^{-1} and 1028 cm^{-1} with thio (2689 cm^{-1}) (refer Figure 7). Besides, the appearance of other functional group also signified the formation of the NPs, such as isothiocyanate (2140 cm^{-1} and 2020 cm^{-1}), aromatic-alkene (1588 cm^{-1}, 1562 cm^{-1} and 940 cm^{-1}), and benzene functional groups (1380 cm^{-1}) (Tajau et al., 2020).

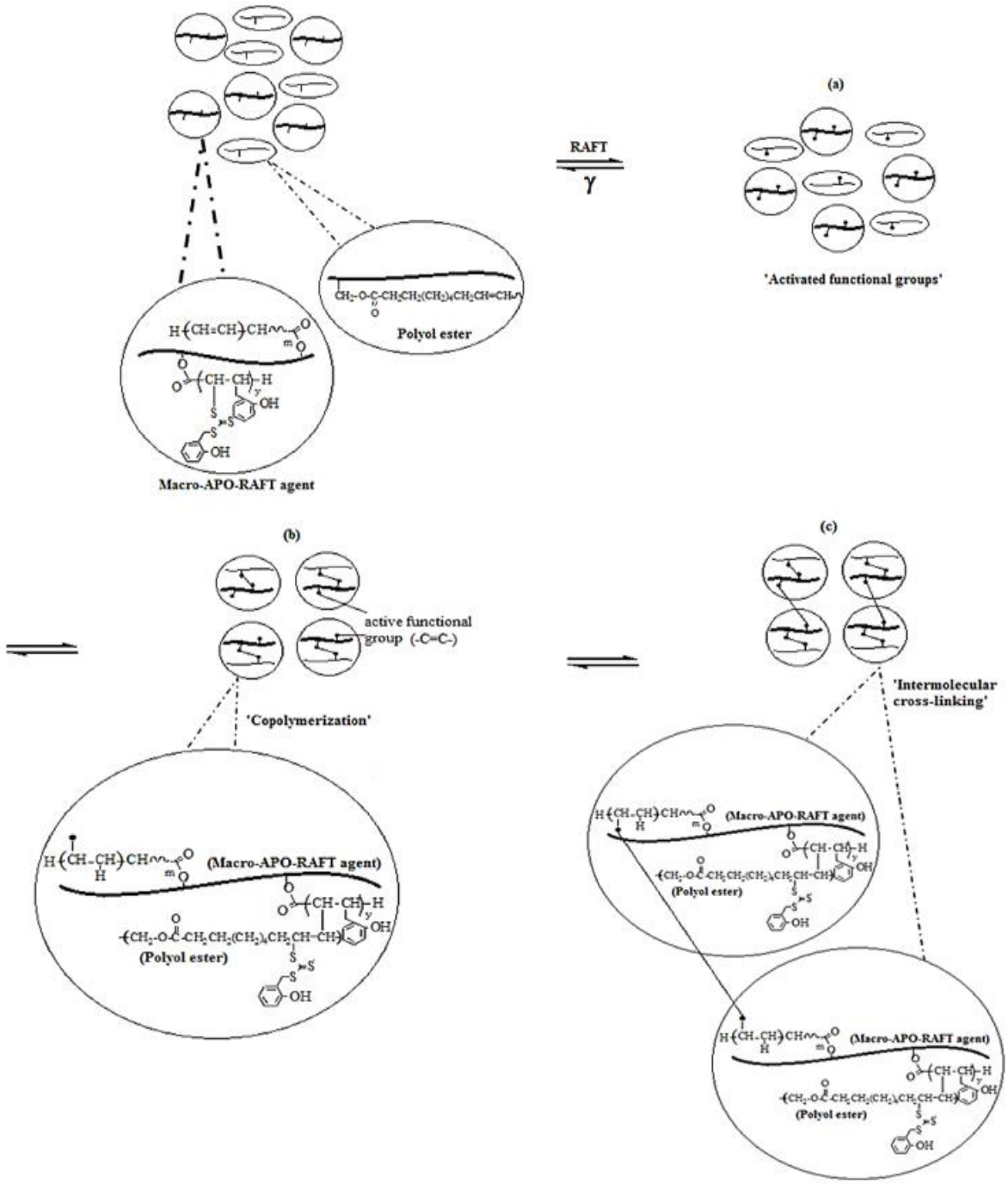

Figure 1: Schematic diagram of the RAFT polymerisation and crosslinking process of poly(APO-*b*-polyol ester) NPs throughout the application for radiation by using a gamma source

Percentage of reactants conversion to macro-APO-RAFT agent and nanoparticles

The use of UV-Vis spectrophotometer showed that the 0.001022 M radical concentration level from 500 Gy dosage as being necessary to form the molecular weight of up to 16.36 kDa, as shown in Table 1. Therefore, this dosage was selected for the production of macro-APO-RAFT agent. It was reported that RAFT polymerisation was more controllable by increasing the monomer concentration, while reducing molecular weight means reducing the RAFT polymerisation process (Zhang et al., 2017).

Table 2 indicates the actual amount of APO or DBTTC RAFT agent used in RAFT polymerisation and demonstrates that the dosage of 500 Gy was the ultimate dosage to produce a macro-APO-RAFT agent.

Furthermore, the dose of gamma radiation at 700 Gy was described as the appropriate dose for the creation of NPs with a weight-average MW value of 23.98 kDa. With 3 mg of polyol ester and 1 mg of DBTTC, small nanoparticle dimensions (<150 nm) could be obtained after exposure to gamma irradiation of 700 Gy. Table 3 shows the actual weight and percentage of reactant conversion (APO, polyol ester and DBTTC) for the processing of RAFT polymerisation and crosslinking reactions of NPs under gamma irradiation with stirring speed of 6000 rpm. The polymerisation reaction was efficient and the reactants were found to be an ideal formulation with the percentage conversion of polyol ester monomers at 61.43%. Also, high percentage conversion of APO (98.78%) and DBTTC (99.99%) used for generating NPs. The model production NPs yield at a dose of 700 Gy gamma irradiation was 81.45% (±2.57), contributing to an effective RAFT polymerisation and crosslinking, as calculated by using Equation 8.

Table 1: A comparison of the concentration and average molecular weights between the macro-APO radicals and the absorbed dose

Dose, Gy	GPC technique	UV-Vis spec technique
	Average molecular weight, kDa	Concentration, Mol/L
0	6.25	0.001009
500	16.36	0.001022
700	12.88	0.001014

Table 2: Actual amount of APO and DBTTC used to generate the macro-APO-RAFT agent

Dose (Gy)	Irradiation time (s)	Initial weight of APO (mg/L)	Actual weight of APO usage (mg/L)	Initial weight of DBTTC (mg/L)	Actual weight of DBTTC usage (mg/L)
0	0	180	176.5961	3	2.9984
500	900	180	178.9235	3	2.9992
700	1260	180	177.5123	3	2.9986

Table 3: Actual amount of APO, polyol ester and DBTTC in generating the NPs

Sample: (Polyol ester/ DBTTC) (mg)	Size (nm)	Optimum Dose (Gy)	APO (mg/L)			Polyol ester (mg/L)			DBTTC (mg/L)		
			Initial weight	Actual weight usage	Percen -tage usage (%)	Initial weight	Actual weight usage	Percen -tage usage (%)	Initial weight	Actual weight usage	Percen -tage usage (%)
(3/ 1)	142.09	700	180	177.81	98.78	3	1.843	61.43	1	0.9999	99.99

Particle size and morphology

As shown in Figure 2b, the significant increase of particle size at 142.09 nm was observed at 700 Gy that was resulted from the reactive copolymerisation and the intermolecular crosslinking processes. Consequently, the degradation experienced by the copolymers NPsnetwork structure from a further increase of the irradiation dose at 1 kGy, 5 kGy and 10 kGy (Figure 2a) (IAEA 2004, 2009; Tajau et al., 2020). This was substantiated by the optimum irradiation dose in the poly(APO-*b*-polyol ester) NPs synthesis could be regarded as the factor that influencing the decrease of the nanoparticle size at

a higher dosage level. The size of the NPs was also identified by using FESEM and the images are presented in Figure 2c. Figure 2c shows the spherical NPs formed and the mean particle size distribution at 76.98 nm.

DLS obtained hydrodynamic particle size based on the diffusion of the nanoparticle, which was measured from the inner and outer layer of the nanoparticle in wet condition as it was immersed in fluid. FESEM measurement was based on the response of the electron dense phase or inner core of the nanoparticle that provided the actual dehydrated (dry) nanoparticle size. Therefore, the NPs size obtained via FESEM was expected and proven to be smaller than DLS, since the hydration or outer layer of the particles was basically absent (Niu et al., 2018).

The produced NPs possessed a common polymeric particle size of 10 nm−1000 nm for drug delivery system as reported in many studies (Bennet & Kim, 2014; Bolhassani et al., 2014; De Jong & Borm, 2008; Han, J. et al., 2018; Lombardo et al., 2019; Nagavarma et al., 2012).

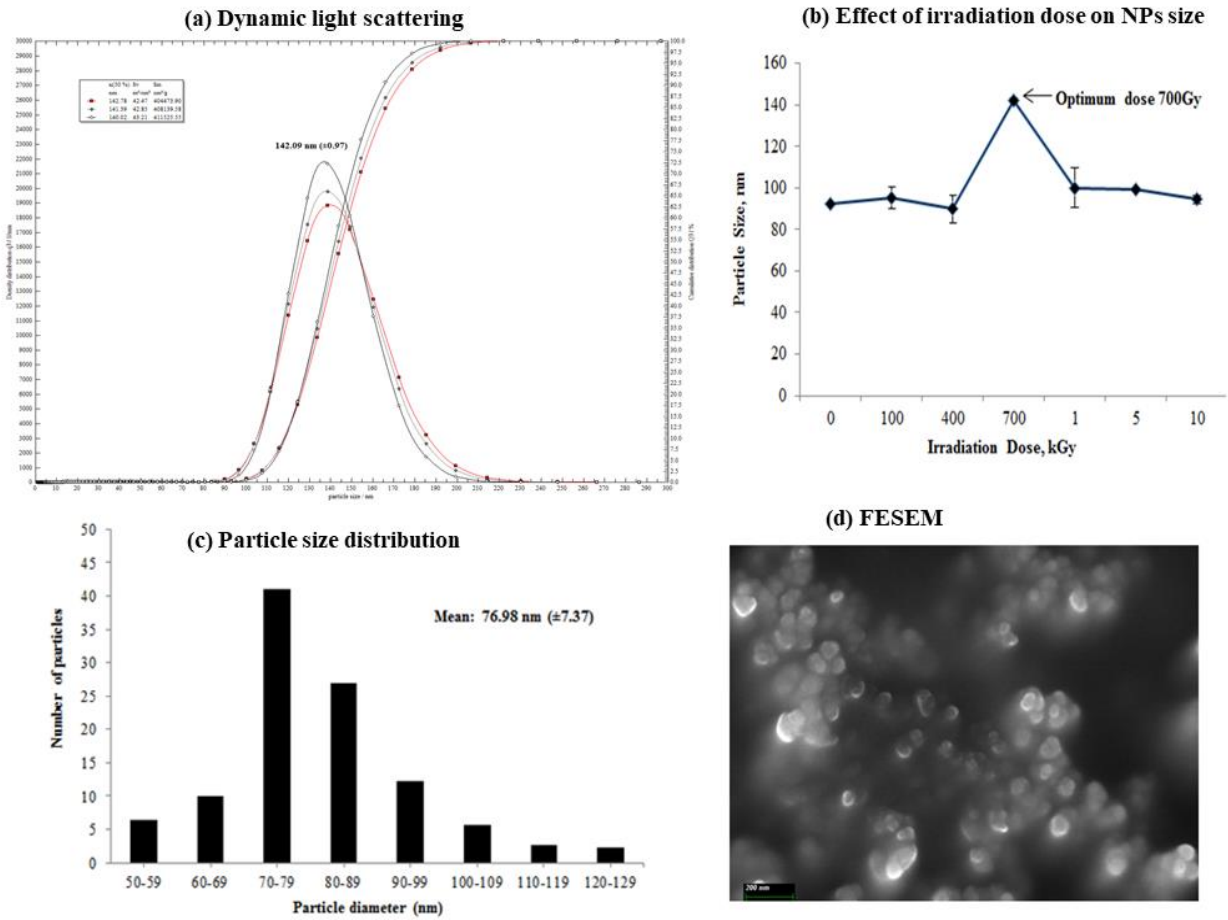

Figure 2:
(a) Particle size distribution measured by dynamic light scattering,
(b) Effect of the hydrodynamic particle diameter from the gamma irradiation dose on the formation of the poly(APO-*b*-polyol ester) NPs (Tajau et al., 2020),
(c) The particle size distribution of poly(APO-*b*-polyol ester) NPs,
(d) FESEM micrograph of poly(APO-b-polyol ester) NPs irradiated at 700 Gy.

Thermal and amorphous properties

The thermal stability of the NPs was identified by using the TGA and decomposition curves of samples are shown in TGA and DTA curves, as shown in Figure 3. The NPs showed four stages of decomposition curves. At the initial stage of 212.46 °C, the curve contributed to the dehydration of moisture and volatile compounds at 22.40% of weight loss (Figure 3, TGA curve). This dehydration peak also was detected at 47.51 ^{o}C in the DTA curve. At the second stage region of 286 °C, the degradation curve contributed the breaking of hydrocarbon bonds of the copolymer network between APO and the polyol ester with 18.30% of weight loss, whereas it was not shown in the raw polyol ester (Tajau et al., 2018) and raw APO thermogram. In the following temperature of 378.97 ^{o}C, the weight loss was attributed to the loss of ester at 50.10% (Tajau et al., 2018). The region above 473.34 ^{o}C was contributed to the loss of alkyl groups with 9.20% of weight loss (Figure 3).

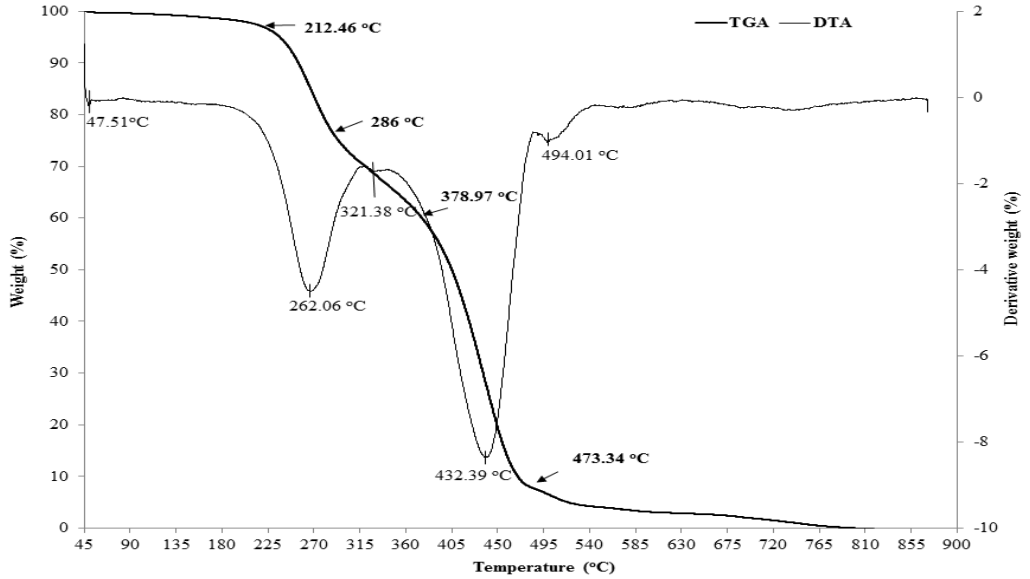

Figure 3: The TGA thermogram of the poly(APO-*b*-polyol ester) NPs irradiated at 700 Gy

DSC analysis was also used to measure the thermal characteristic of the poly(APO-*b*-polyol ester) NPs (Figure 4). For the first heating scan process, a small broad peak was found at 38.20 ^{o}C, whereas the second scan did not show this moisture peak. A similar observation was revealed in the DTA curve in Figure 3, whereby this moisture peak occurred at temperature of 47.51 ^{o}C and was related to the loss of a part of bound water phenomenon (Figure 4).

Furthermore, there were two temperature peaks identified signifying the formation of saturated triacylglycerols (TAG) crystal. For the first cooling process, the crystallisation peak occurred at 52.61 ^{o}C, followed by the second peak at 3.92 ^{o}C. When recooled, the first crystallisation peak occurred at 49.03 ^{o}C and the second peak occurred at 3.09 ^{o}C. These TAG crystal peaks were due to the presence of diglycerides structure and composition from the APO. In the different circumstances, the molten TAG-crystal was obtained by the melting curves which showed broad and short peaks. The results showed two melting peaks in each melting curve: at 9.07 ^{o}C and 75.38 ^{o}C for the first scan and when remelted at 9.37 ^{o}C and 75 ^{o}C, which corresponded to the polymorphic transition of the TAGs during the crystal melting.

However, these crystallisation and melting curves were not representing the real apparent of the crystal-like common semi-crystalline or crystalline polymers because the melting curves did not possess a sharp melting point (Figure 4). From the XRD graph in Figure 5, the percentage of crystalinity of the poly(APO-*b*-polyol ester) NPs was calculated at 1.92%, which indicated a very

slightly of the crystal contained. Therefore, the poly(APO-*b*-polyol ester) NPs tended to display amorphous characteristics. Therefore, many studies had reported that the new synthesised polymer compounds derived from the palm oil-based materials via polymerisation or blending tended to promote a random or amorphous distribution of a new polymer structure. In this study, the poly(APO-*b*-polyol ester) NPs demonstrated an amorphous property that indicated better aqueous solubility than the crystalline material (Jadhav et al., 2009).

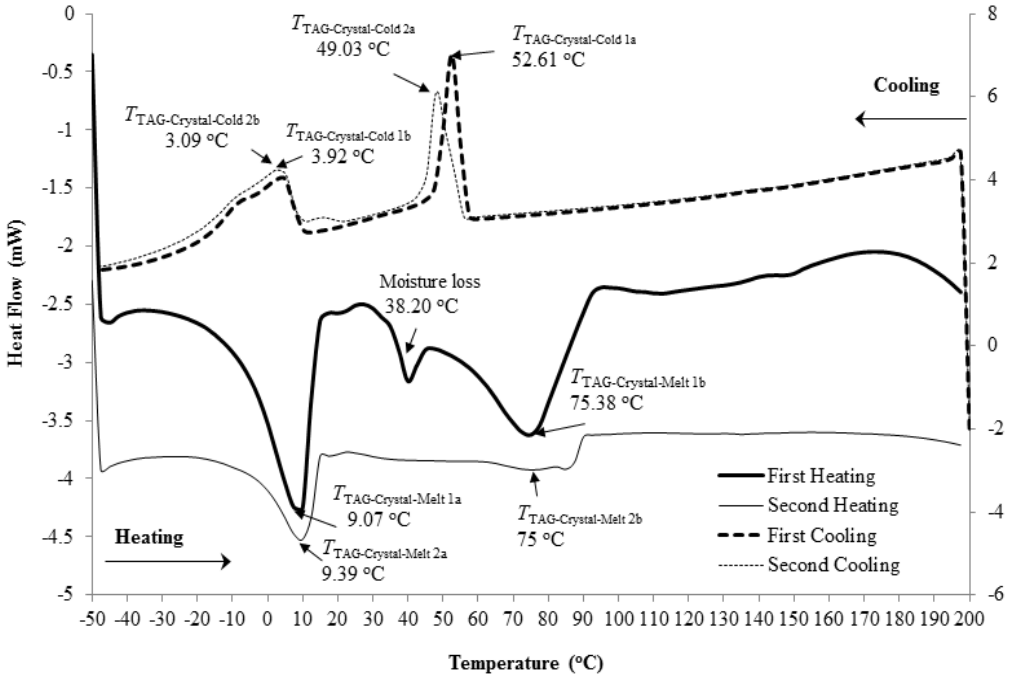

Figure 4: The DSC thermogram of the poly(APO-*b*-polyol ester) NPs irradiated at 700 Gy

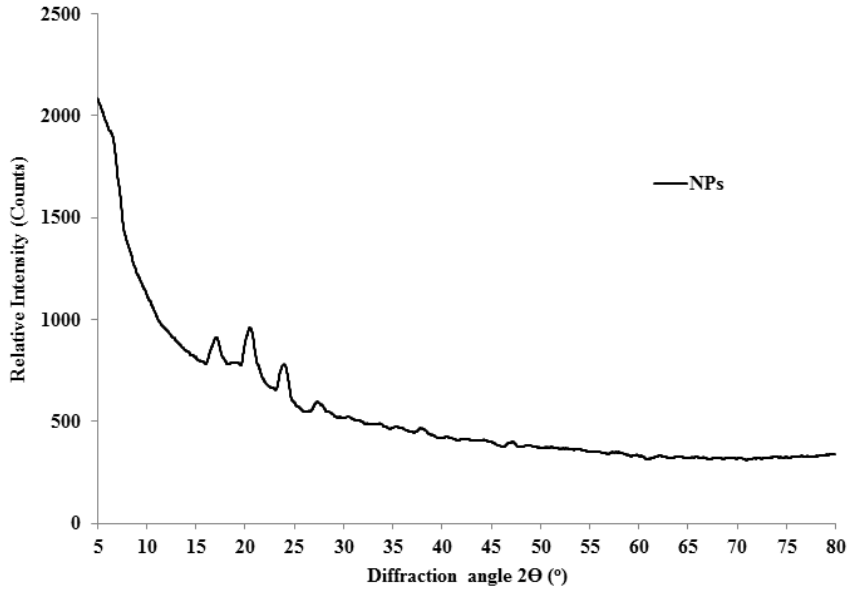

Figure 5: The XRD pattern of the poly(APO-*b*-polyol ester) NPs irradiated at 700 Gy

Biodegradability

Figure 6 reveals that the structure of NPs collapsed significantly during the 30-day degradation period as opposed to the fine form of NPs structure before the degradation process (Figure 2(b)). Figure 6 reveals the TEM image showed after 60 and 90 days, whereby the NPs kept degrading. The FTIR spectral peaks shown in Figure 7 indicated that the major compounds that caused of degradation were the hydrolysable ester bonds, such as -OH of hydroxyl group, -C=O of carbonyl, and C-O-O and C-O of ester groups (Luginina et al., 2020; Tajau et al., 2020).

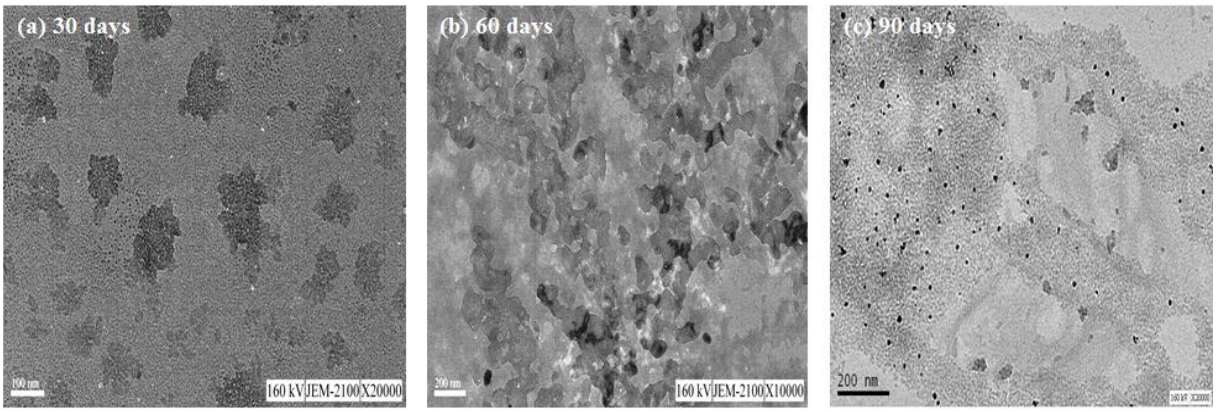

Figure 6: TEM images of dried poly(APO-*b*-polyol ester) NPs after degradation

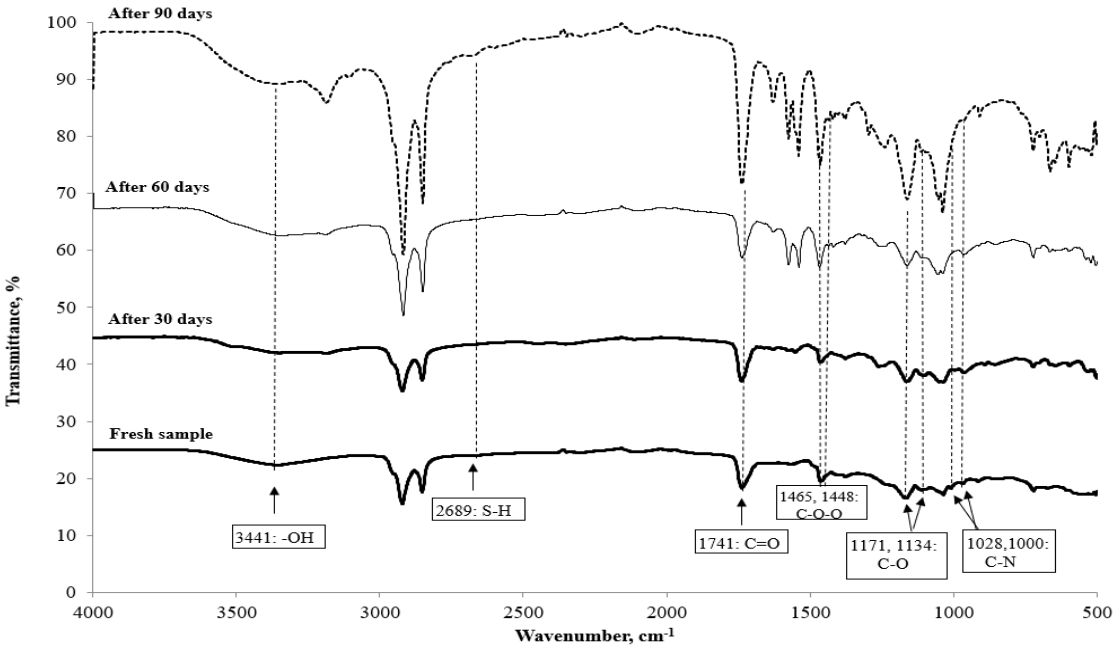

Figure 7: FTIR spectra of poly(APO-*b*-polyol ester) NPs under degradation process in SBF solution for 30 days, 60 days and 90 days at 37 ºC

CONCLUSION

In conclusion, this study found that the suggested gamma radiation-induced RAFT polymerisation technique to be not only useful and well-adapted for use in the poly(APO-*b*-polyol ester) NPs synthesis, but also an environmentally friendly approach in generating the desired NPs due to the absence of initiators and catalysts in its process. It was also observed that the hydrolysed ester bond of these poly(APO-*b*-polyol ester) NPs had very good biodegradable properties, as shown in the TEM

study. In addition, the hydrodynamic particle having diameter of less than 150 nm when exposed to a very brief gamma irradiation exposure of 700 Gy. Since these physicochemical properties are essential for a more effective drug delivery system, as well as applications in the scaffolding and implants of the biomedical. The environmentally friendly gamma radiation induced-RAFT polymerisation technique used in this study could then offer a more economical and sustainable source in the development of the targeted polymeric NPs.

ACKNOWLEDGEMENTS

The authors gratefully acknowledged the Malaysian Nuclear Agency for their materials and instruments support under the Radiation Processing Technology Division (Project code: NM-R&D-15-01). The authors would also like to extend their appreciation for the support given by the Department of Chemical and Process Engineering (JKKP), Universiti Kebangsaan Malaysia (UKM). This research was funded by UKM (DIP/2019/012), Malaysian Ministry of Higher Education (FRGS/1/2018/TK02/UKM/02/2) and Public Service Department (JPA) (Scholarship/HLP/2016).

REFERENCES

Ashfaq, A., Clochard M.C., Coqueret, X., Dispenza, C., Driscoll, M. S., Ulański, P. & Al-Sheikhly, M. (2020). Polymerization Reactions and Modifications of Polymers by Ionizing Radiation. *Polymers (Basel)* 12(12): 2877.

Barner, L., Quinn, J. F., Barner-Kowollik, C. Vana, P. & Davis, T.M. (2003). Reversible addition-fragmentation chain transfer polymerization initiated with γ- radiation at ambient temperature: An overview. *European polymer journal* 39, 449-459.

Barsbay, M. & Güven, O. (2020). Nanostructuring of polymers by controlling of ionizing radiation-induced free radical polymerization, copolymerization, grafting and crosslinking by RAFT mechanism. *Radiation Physics and Chemistry* 169.

Bennet, D. & Kim, S. (2014). Polymer nanoparticles for smart drug delivery. *Application of Nanotechnology in Drug Delivery* pp. 258-310.

Bolhassani, A., Javanzad, S., Saleh, T., Hashemi, M., Aghasadeghi, M.R. & Sadat, S.M. (2014). Polymeric nanoparticles: Potent vectors for vaccine delivery targeting cancer and infectious diseases. *Human Vaccines & Immunotherapeutics* 10(2), 321-332.

Bowes, A. (2007). *Novel synthesis of block copolymers via the RAFT process.* Stellenbosch: University of Stellenbosch.

Chen, J. & Seko, N. (2017). Effects of raft agent on the chloromethylstyrene polymerizations in a simultaneous radiation grafting system. *Polymers* 9(8), 307.

Chiefari, J., Chong, Y. K., Ercole, F., Krstina, J., Jeffery, J., Le, T. P. T., Mayadunne, R.T.A., Meijs, G.F., Moad, C.L., Moad, G., Rizzardo, E. & Thang, S. H. (1998). Living free-radical polymerization by reversible addition-fragmentation chain transfer. *Macromolecules* 31, 5559-5562.

De Jong, W.H. & Borm, P.J.A. (2008). Drug delivery and nanoparticles: Applications and hazards. *International Journal of Nanomedicine* 3(2), 133-149.

Flores-Rojas, G.G., López-Saucedo, F. & Bucio, E. (2020). Gamma-irradiation applied in the synthesis of metallic and organic nanoparticles: A short review. *Radiation Physics and Chemistry* 169,107962.

Güven, O. (2021). RadiationAssisted Synthesis of Polymer-Based Nanomaterials. *Appl. Sci.* 11, 7913.

Han, J., Zhao, D., Li, D., Wang, X., Jin, Z. & Zhao, K. (2018). Polymer-based nanomaterials and applications for vaccines and drugs. *Polymers* 10(31), 1-14.

IAEA. (2004). Advances in Radiation Chemistry of Polymers. *International Atomic Energy Agency.*

IAEA. (2009). Controlling of Degradation Effects in Radiation Processing of Polymers. *International Atomic Energy Agency* pp. 1-225.

IAEA. (2010). Nanoscale Radiation Engineering of Advanced Materials for Potential Biomedical Applications. *International Atomic Energy Agency.*

IAEA. (2002). Radiation Synthesis and Modification of Polymers for Biomedical Applications. *International Atomic Energy Agency.*

Jadhav, N. R., Gaikwad, V. L., Nair, K. J. & Kadam, H. (2009). Glass transition temperature: Basics and application in pharmaceutical sector. *Asian Journal of Pharmaceutics* 3(8), 82-89.

Lombardo, D., Kiselev, M.A. & Caccamo, M.T. (2019). Smart nanoparticles for drug delivery application: development of versatile nanocarrier platforms in biotechnology and nanomedicine. *Journal of Nanomaterials* 1-26.

Luginina, M., Schuhladen, K., Orrú, R., Cao, G., Boccaccin, A.R. & Liverani, L. (2020). Electrospun PCL/PGS composite fibers incorporating bioactive glass particles for soft tissue engineering applications. *Nanomaterials* 10(978), 1-18.

Meléndez-Ortiz, H. I., Varca, G. H. C., Lugão, A. B. & Bucio, E. (2015). Smart polymers and coatings obtained by ionizing radiation: Synthesis and biomedical applications. *Open Journal of Polymer Chemistry* 5, 17-33.

Millard, P. E., Barner, L., Reinhardt, J., Buchmeiser, M. R., Barner-Kowollik, C. & Müller, A. H. E. (2010). Synthesis of water-soluble homo- and block-copolymers by RAFT polymerization under γ-irradiation in aqueous media. *Polymer* 51(19), 4319-4328.

Moad, G., Rizzardo, E. & Thang, S. H. (2006). Living radical polymerization by the RAFT process-A first update. *Australian Journal of Chemistry* 59, 669-692.

Nagavarma, B.V.N., Yadav, H.K.S., Ayaz, A., Vasudha, L.S. & Shivakumar, H.G. (2012). Different techniques for preparation of polymeric nanoparticles- A review. *Asian Journal of Pharmaceutical and Clinical Research* 5(3), 16-23.

Niu, S., Bremner, D.H., Wu, J., Wu, J., Wang, H., Li, H., Qian, Q., Zheng, H. & Zhu, L. (2018). l-Peptide functionalized dual-responsive nanoparticles for controlled paclitaxel release and enhanced apoptosis in breast cancer cells. *Drug Delivery* 25(1), 1275-1288.

Quinn, J. F., Davis, T. P., Barner, L. & Barner-Kowollik, C. (2007). The application of ionizing radiation in reversible additionefragmentation chain transfer (RAFT) polymerization: Renaissance of a key synthetic and kinetic tool. *Polymer* 48 6467-6480.

Rosiak, J. M., Janik, I., Kadlubowski, S., Kozicki, M., Kujawa, P., Stasica, P. & Ulanski, P. (2002). Radiation Formation of Hydrogels for Biomedical Application. *International Atomic Energy Agency.*

Stenzel, M. H. (2008). RAFT polymerization: an avenue to functional polymeric micelles for drug delivery. *Chemical Communications* 3486-3503.

Tajau, R., Hashim, K., Sharif, J. & Ratnam, C.T. (2017). *Teknologi Pemprosesan Sinaran Mengion [Ionizing Radiation Processing Technology]*. Selangor: Dewan Bahasa dan Pustaka.

Tajau, R., Rohani, R. & Salleh, M. Z. (2020). Physicochemical and thermal properties of acrylated palm olein as promising biopolymer. *Journal of Polymers and the Environment* 1-15.

Tajau, R., Rohani, R., Abdul Hamid, S.S., Adam, Z., Mohd Janib, S.N. & Salleh M.Z. (2020). Surface functionalisation of poly APO b polyol ester cross linked copolymers as core–shell nanoparticles for targeted breast cancer therapy. *Scientific Reports* 10 (21704), 1-17.

Tajau, R., Rohani, R., Wan Isahak, W.N.R., Salleh, M.Z. & Ghazali, Z. (2018). Development of new bio-based polyol ester from palm oil for potential polymeric drug carrier. *Advances in Polymer Technology* 1-9.

Tian, X., Ding, J., Zhang, B., Qiu, F., Zhuang, X. & Chen, Y. (2018). Recent advances in raft polymerization: Novel initiation mechanisms and optoelectronic applications. *Polymers* 10(318), 1-26.

Ulanski, P. & Rosiak, J. M. (2004). Polymeric nano/microgels. *Encyclopedia of Nanoscience and Nanotechnology*, (Vol. x, pp. 1-26). Los Angeles: American Scientific Publishers.

Ulanski, P. & Rosiak, J. M. (1999). The use of radiation technique in the synthesis of polymeric nanogels. *Journal of Nuclear Instruments and Methods in Physics Research (B)* 151, 356-360.

Zhang, S., Yin, L., Wang, J., Zhang, W., Zhang, L. & Zhu, X. (2017). A green platform for preparation of thewell-defined polyacrylonitrile: 60Co gamma-ray irradiation-initiated raft polymerization at room temperature. *Polymers* 9(26), 1-10.